

## RESEARCH ARTICLE

# Is vertebral shape variability in caecilians (Amphibia: Gymnophiona) constrained by forces experienced during burrowing?

Aurélien Lowie<sup>1,‡</sup>, Barbara De Kegel<sup>1</sup>, Mark Wilkinson<sup>2</sup>, John Measey<sup>3</sup>, James C. O'Reilly<sup>4</sup>, Nathan J. Kley<sup>5</sup>, Philippe Gaucher<sup>6</sup>, Jonathan Brecko<sup>7</sup>, Thomas Kleinteich<sup>8</sup>, Dominique Adriaens<sup>1,\*</sup> and Anthony Herrel<sup>1,9,\*</sup>

## ABSTRACT

Caecilians are predominantly burrowing, elongate, limbless amphibians that have been relatively poorly studied. Although it has been suggested that the sturdy and compact skulls of caecilians are an adaptation to their head-first burrowing habits, no clear relationship between skull shape and burrowing performance appears to exist. However, the external forces encountered during burrowing are transmitted by the skull to the vertebral column, and, as such, may impact vertebral shape. Additionally, the muscles that generate the burrowing forces attach onto the vertebral column and consequently may impact vertebral shape that way as well. Here, we explored the relationships between vertebral shape and maximal *in vivo* push forces in 13 species of caecilian amphibians. Our results show that the shape of the two most anterior vertebrae, as well as the shape of the vertebrae at 90% of the total body length, is not correlated with peak push forces. Conversely, the shape of the third vertebrae, and the vertebrae at 20% and 60% of the total body length, does show a relationship to push forces measured *in vivo*. Whether these relationships are indirect (external forces constraining shape variation) or direct (muscle forces constraining shape variation) remains unclear and will require quantitative studies of the axial musculature. Importantly, our data suggest that mid-body vertebrae may potentially be used as proxies to infer burrowing capacity in fossil representatives.

**KEY WORDS:** Axial skeleton, Geometric morphometrics, Post-cranial, Push force

## INTRODUCTION

Caecilians (Gymnophiona) are a small (about 215 currently recognized species) monophyletic group of elongate, totally


limbless and annulated amphibians. Because most caecilians are strongly fossorial, inconspicuous and rarely encountered components of tropical ecosystems, many aspects of their biology remain poorly known (O'Reilly, 2000; Summers and O'Reilly, 1997; Wilkinson, 2012). Although their cranial osteology has been relatively well documented (e.g. Bardua et al., 2019; Lowie et al., 2021; Sherratt et al., 2014; Wake, 1993; Wilkinson and Nussbaum, 1997), few studies have focused upon the postcranial morphology of adult extant caecilians (but see Lowie et al., 2022b; Peter, 1894; Renous and Gasc, 1989; Renous et al., 1993; Taylor, 1977; Wake, 2003, 1980, Wiedersheim, 1879).

In direct association with their burrowing habits, it is thought that caecilian skull evolution resulted in compact and robust skulls with many bones being fused or connected through tight sutures (Nussbaum and Pfreder, 1998; Taylor, 1968; Wake, 1993; Wake and Hanken, 1982). Unexpectedly, however, previous studies on the impact of burrowing force on skull shape suggested that there is no direct relationship between the external forces experienced during burrowing and skull shape (Ducey et al., 1993; Herrel and Measey, 2010; Kleinteich et al., 2012; Lowie et al., 2021). Rather, cranial shape variation appears more constrained by the jaw adductor muscles in relation to feeding (Lowie et al., 2022a). However, the external forces encountered during burrowing are transmitted by the head to the vertebral column and could therefore impact vertebral form and function. Moreover, a recent study by Lowie et al. (2022b) demonstrated that variation in vertebral form occurs along the vertebral column, suggesting that not all vertebrae may be impacted similarly by the constraints imposed by a head-first burrowing lifestyle.

As far as is known, most caecilians are capable of moving through narrow tunnels using a combination of hydrostatic and internal concertina locomotion (Gaymer, 1971; O'Reilly et al., 1997; Herrel and Measey, 2012; Summers and O'Reilly, 1997), thanks to a partial independence between the vertebral column and the skin with the associated external muscular sheath of the body (Naylor and Nussbaum, 1980; Nussbaum and Naylor, 1982). During internal concertina locomotion, the vertebral column is flexed inside the body to provide purchase against the substrate, while the head and anterior-most vertebrae remain largely extended. The waves created by the vertebral column then progressively straighten and the animal pushes its head into the soil (Gans, 1973; Gaymer, 1971; Herrel and Measey, 2012; Summers and O'Reilly, 1997). Whereas we anticipate that the shape of the anterior vertebrae is likely strongly impacted by the reaction forces incurred while pushing the head into the substrate, the mid-body and more posterior vertebrae are likely more impacted by the axial musculature that generates the forces used to push the head forward into the soil.

<sup>1</sup>Department of Biology, Evolutionary Morphology of Vertebrates, Ghent University, K.L. Ledeganckstraat 35, 9000 Gent, Belgium. <sup>2</sup>Department of Life Sciences, Natural History Museum, London SW7 5BD, UK. <sup>3</sup>Centre for Invasion Biology, Department of Botany & Zoology, Stellenbosch University, Private Bag X1, 7602 Matieland, Stellenbosch, South Africa. <sup>4</sup>Department of Biomedical Sciences, Ohio University, Cleveland Campus, SPS-334C, Cleveland, OH 45701, USA. <sup>5</sup>Department of Anatomical Sciences, Health Sciences Center, T8-082, Stony Brook University, Stony Brook, NY 11794-8081, USA. <sup>6</sup>USR 3456, CNRS, Centre de recherche de Montabo IRD, CNRS-Guyane, 97334 Cayenne, French Guiana. <sup>7</sup>Royal Museum for Central Africa, Biological Collections and Data Management, 3080 Tervuren, Belgium. <sup>8</sup>TPW Prufzentrum GmbH, 41460 Neuss, Germany. <sup>9</sup>UMR 7179 C.N.R.S./M.N.H.N., Département d'Ecologie et de Gestion de la Biodiversité, 57 rue Cuvier, Case postale 55, 75231, Paris Cedex 5, France. \*Co-last authors

<sup>‡</sup>Author for correspondence (aurelien.lowie@UGent.be)

 A.L., 0000-0003-0065-7152; J.M., 0000-0001-9939-7615; A.H., 0000-0003-0991-4434

In this study, we explored whether vertebral shape is associated with the peak push forces measured *in vivo* for 13 species of caecilian amphibians (Lowie et al., 2021). We predicted that, globally, the higher push forces produced by active burrowers will be associated with more robust vertebrae. We also expected to find a stronger relationship between burrowing force and vertebral shape in the anterior part of the body, as forces are likely dissipated further down the vertebral column. Alternatively, relationships between the external forces and vertebral shape may be more indirect, with the muscles generating the force constraining vertebral shape. In that case, relationships between force and shape would be expected to be strongest for the mid-body vertebrae.

## MATERIALS AND METHODS

### Specimens

On the basis of vertebral anatomy alone, only a cervical region can be identified unambiguously in all caecilians; post-cervical body regions cannot be precisely delineated solely on the basis of vertebral characters (Wake, 1980, 2003). Caecilians generally have an atlas followed by 67 (*Hypogeophis pti*; Maddock et al., 2017) to 306 (*Oscacilia cf. bassleri*; M.W., personal observation) trunk vertebrae with no sacrum and either a short tail or no tail at all (Dunn, 1942; Maddock et al., 2017; Nussbaum and Wilkinson, 1989). To be able to compare vertebral shape across species that differ in vertebral number, we followed Wake (1980) in selecting six vertebrae: the atlas (V1), the second vertebra (V2), the third vertebra (V3), and the vertebrae at 20% (hereafter referred to as V20%), 60% (hereafter referred to as V60%) and 90% (hereafter referred to as V90%) of the total number of vertebrae. This selection was made under the assumption that all caecilians included in our study have a sufficiently similar vertebral organization. For the atlas (V1), shape was quantified for 53 individuals from 13 species belonging to eight of the 10 currently recognized families. For the five other vertebrae of interest, the dataset consisted of 40 individuals from 13 species based on the availability of whole-body micro-computed tomography ( $\mu$ CT) scans of high resolution (Table 1). Our sample was restricted to adults and included both males and females. Although some sexual dimorphism is present in caecilians (e.g. Kupfer, 2009; Maerker et al., 2016), interspecific variation largely exceeds sex-specific variation (Sherratt et al., 2014). Specimens were obtained primarily from our personal collections and completed with specimens from museum collections (Table S1).

**Table 1. Details of specimens of caecilian amphibians (Gymnophiona) used in this study**

Family	Species	N atlas	N vertebrae
Rhinatrematidae	<i>Rhinatremata bivittatum</i>	5	3
Ichthyophiidae	<i>Ichthyophis kohtaoensis</i>	4	3
Herpeliidae	<i>Boulengerula fischeri</i>	5	4
	<i>Boulengerula taitanus</i>	5	3
Caeciliidae	<i>Herpele squalostoma</i>	5	5
	<i>Caecilia museugoeldi</i>	1	1
	<i>Caecilia tentaculata</i>	2	2
Typhlonectidae	<i>Typhlonectes compressicauda</i>	5	3
Indotyphlidae	<i>Hypogeophis rostratus</i>	4	3
Siphonopidae	<i>Siphonops annulatus</i>	3	1
Dermophiidae	<i>Dermophis mexicanus</i>	4	4
	<i>Geotrypetes seraphini</i>	6	4
	<i>Schistometopum thomense</i>	4	4

N indicates the number of individuals for each dataset.

### $\mu$ CT imaging

About half of the  $\mu$ CT scans used were generated at the Centre for X-Ray Tomography at Ghent University, Belgium (UGCT, www.ugct.ugent.be) using the HECTOR  $\mu$ CT scanner (Masschaele et al., 2013). The scanner settings were sample dependent. The tube voltage varied between 100 and 120 kV and the number of X-ray projections taken over 360 deg was typically about 2000 per scan. Additional  $\mu$ CT scans were obtained from the online repository Morphosource (morphosource.org), the Zoological Museum Hamburg (see Kleinteich et al., 2008, for scanner settings), the Royal Museum of Central Africa (75 kV, 1440 projections) and the Natural History Museum, London (mostly 100 kV, 3142 projections; see Table S1). The isotropic voxel sizes of all scans are listed in Table S1. All the  $\mu$ CT scans were processed using both automatic thresholding and manual segmentation to reconstruct the vertebrae in 3D using Amira 2019.3 (Visage Imaging, San Diego, CA, USA). Using Geomagic Wrap (3D systems), surfaces were prepared by removing highly creased edges and spikes that might have interfered with the placement of landmarks.

### 3D geometric morphometrics

All anatomical landmarks were placed by the same person (A.L.) using Stratovan Checkpoint (Stratovan corporation, v.2020.10.13.0859). Nineteen homologous landmarks were placed on each atlas, whereas 22 homologous landmarks were placed on the other vertebrae included in our analyses (see Lowie et al., 2022b, for more information). Generalized Procrustes analyses (GPA) were performed on vertebrae using the 'gpgagen' function in the geomorph R package v 3.3.1 (https://CRAN.R-project.org/package=geomorph). Finally, prior to the analyses, asymmetry was removed from the datasets by extracting the symmetric component of shape variation using the 'bilat.symmetry' function of the geomorph package.

### Burrowing force

*In vivo* burrowing forces were measured in the lab or the field for 120 specimens belonging to 13 species (see Lowie et al., 2021; Table 2). Specimens were maintained for a maximum of 24 h in large containers filled with substrate collected in the field at sites where the animals were found. After measurement, animals captured in the field were released at the exact locations where

**Table 2. Number of individuals and maximum resultant push force for the species of caecilian amphibians (Gymnophiona) included in this study**

Species	N	Mean max. push force (N)	Min. push force (N)	Max. push force (N)
<i>Rhinatremata bivittatum</i>	11	0.89±0.52	0.38	2.15
<i>Ichthyophis kohtaoensis</i>	3	4.8±0.72	4.00	5.40
<i>Boulengerula fischeri</i>	8	0.53±0.16	0.34	0.72
<i>Boulengerula taitanus</i>	38	2.56±0.91	0.35	4.69
<i>Herpele squalostoma</i>	7	1.77±1.34	0.55	4.33
<i>Caecilia museugoeldi</i>	2	3.23±0.45	2.92	3.55
<i>Caecilia tentaculata</i>	1	3.88	NA	NA
<i>Typhlonectes compressicauda</i>	15	1.19±0.54	0.28	2.53
<i>Hypogeophis rostratus</i>	2	4.15±1.47	3.11	5.19
<i>Siphonops annulatus</i>	1	6.43	NA	NA
<i>Dermophis mexicanus</i>	8	16.11±4.96	12.72	24.5
<i>Geotrypetes seraphini</i>	12	2.03±0.98	0.52	4.00
<i>Schistometopum thomense</i>	12	1.37±0.62	0.81	3.05

Only adults were included in the dataset. Mean maximum push force values are given as means±s.d.

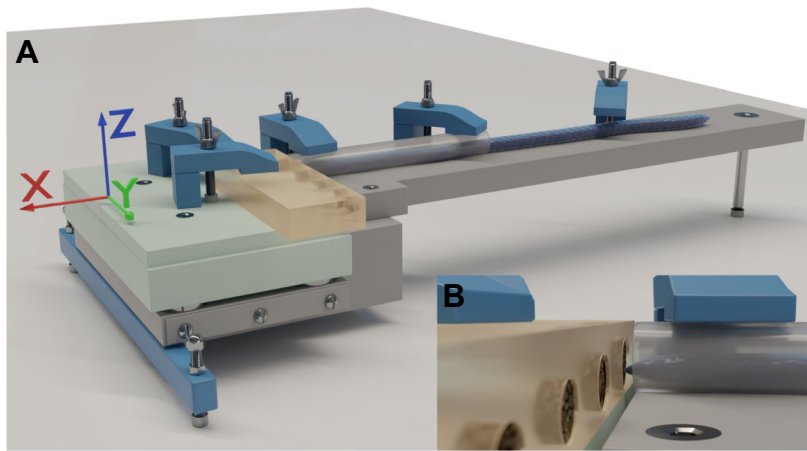


**Fig. 1. Schematic drawing of the set-up used to measure burrowing forces in caecilian amphibians (Gymnophiona).** (A) The specimen was positioned inside the tunnel (transparent) and pushed its head into the soil provided in the Perspex block (orange). The Perspex block was mounted on the force plate (green) recording the force in three directions. The whole set-up was mounted on a purpose-built metal base (gray). (B) Close-up view of the specimen pushing into the Perspex block.

they were found. Push forces were measured using a custom piezoelectric force platform (Kistler Squirrel force plate,  $\pm 0.1$  N; Kistler, Zurich, Switzerland) as described previously (Fig. 1; Herrel et al., 2021; Le Guilloux et al., 2020; Lowie et al., 2021; Vanhooydonck et al., 2011). The force plate was mounted on a purpose-built metal base and connected to a Kistler charge amplifier (type 9865). A Perspex block with 1 cm deep holes of different diameter was mounted on the force plate, level with the front edge. One hole with a diameter corresponding to the body diameter of the animal was filled with substrate from the container of the animal being tested. A tunnel with a diameter equal to the maximum body width of the animal was positioned on the metal base in front of (but not touching) the soil-filled hole in the Perspex block. Then, a caecilian was introduced into the tunnel and allowed to move towards the Perspex block. Next, the animal was stimulated to push into the soil-filled hole by gently tapping the end of its body. Forces were recorded in three dimensions using Bioware software (Kistler) during a 60 s recording session at 500 Hz. Each animal was tested at least 3 times, with an interval of at least 30 min between trials. For each trial, we extracted the forces in the *X*-, *Y*- and *Z*-direction of the best push and calculated the highest peak resultant force. We used the highest peak resultant force across all trials for an animal as an estimate of its maximal push force.

### Phylogeny

Because vertebral data for species are expected to be phylogenetically structured and thus not statistically independent, phylogeny was taken into account in our comparative analyses (Felsenstein, 1985). The phylogenetic tree of Jetz and Pyron (2018) was pruned to only include the species used in our study. Using 10,000 trees from VertLife.org, the maximum credibility tree (Fig. S1) was computed using the 'maxCladeCred' function in the phangorn package in R (<https://CRAN.R-project.org/package=phangorn>).

**Table 3. Results of phylogenetic linear regression between shape and the total number of vertebrae in caecilian amphibians (Gymnophiona)**

Vertebra	$R^2$	<i>P</i> -value
V1	0.04	0.5
V2	0.04	0.5
V3	0.06	0.19
V20%	0.07	0.15
V60%	0.08	0.08
V90%	0.03	0.46

### Statistical analyses

All the statistical analyses were performed in R version 4.0.3 (<http://www.R-project.org/>). The significance threshold (Type I error rate) was set at  $\alpha=0.05$ . Forces were transformed logarithmically ( $\log_{10}$ ) to fulfil assumptions of normality and homoscedasticity.

To estimate the degree of similarity due to shared ancestry, a multivariate *K*-statistic (Adams, 2014) was calculated on the mean Procrustes coordinates of each vertebrae and the external measurements using the 'physignal' function in the geomorph package. A *K*-statistic was calculated on the forces using the 'phylosig' function in the Phytools package (<https://CRAN.R-project.org/package=phytools>). The phylogenetic signal was calculated under the assumption of Brownian motion (Blomberg et al., 2003). The higher the *K*-value, the stronger the phylogenetic signal. Values of  $K>1.0$  describe data with a greater phylogenetic signal than expected from Brownian motion alone.

Phylogenetic generalized least squares (PGLS) regressions were performed using the 'procD.pgls' function from the geomorph package in order to assess (1) the relationship between the total number of vertebrae and their shape, and (2) the relationship between maximum resultant push force and the shape of each vertebra.

### Ethics statement

None of the measurements described in this paper (force measurements) are considered 'procedures' requiring ethics approval under European law. Furthermore, no permits are needed to maintain caecilians in captivity in Europe. All wild-caught animals were maintained for one night and one day, checked for signs of stress and released at their exact site of capture (marked by GPS) the next night. Captive animals were maintained individually in large tubs of soil in a climate-controlled room (24°C) and fed with earthworms and crickets twice weekly. Animals were checked for signs of stress and injury after push force measurements and

**Table 4. Results of phylogenetic linear regression between shape and  $\log_{10}$  burrowing force in caecilian amphibians (Gymnophiona)**

Vertebra	$R^2$	<i>P</i> -value
V1	0.14	0.1
V2	0.11	0.22
V3	0.17	<b>0.05</b>
V20%	0.2	<b>0.04</b>
V60%	0.25	<b>0.04</b>
V90%	0.16	0.12

*P*-values shown in bold are significant at the  $\alpha=0.05$  level.

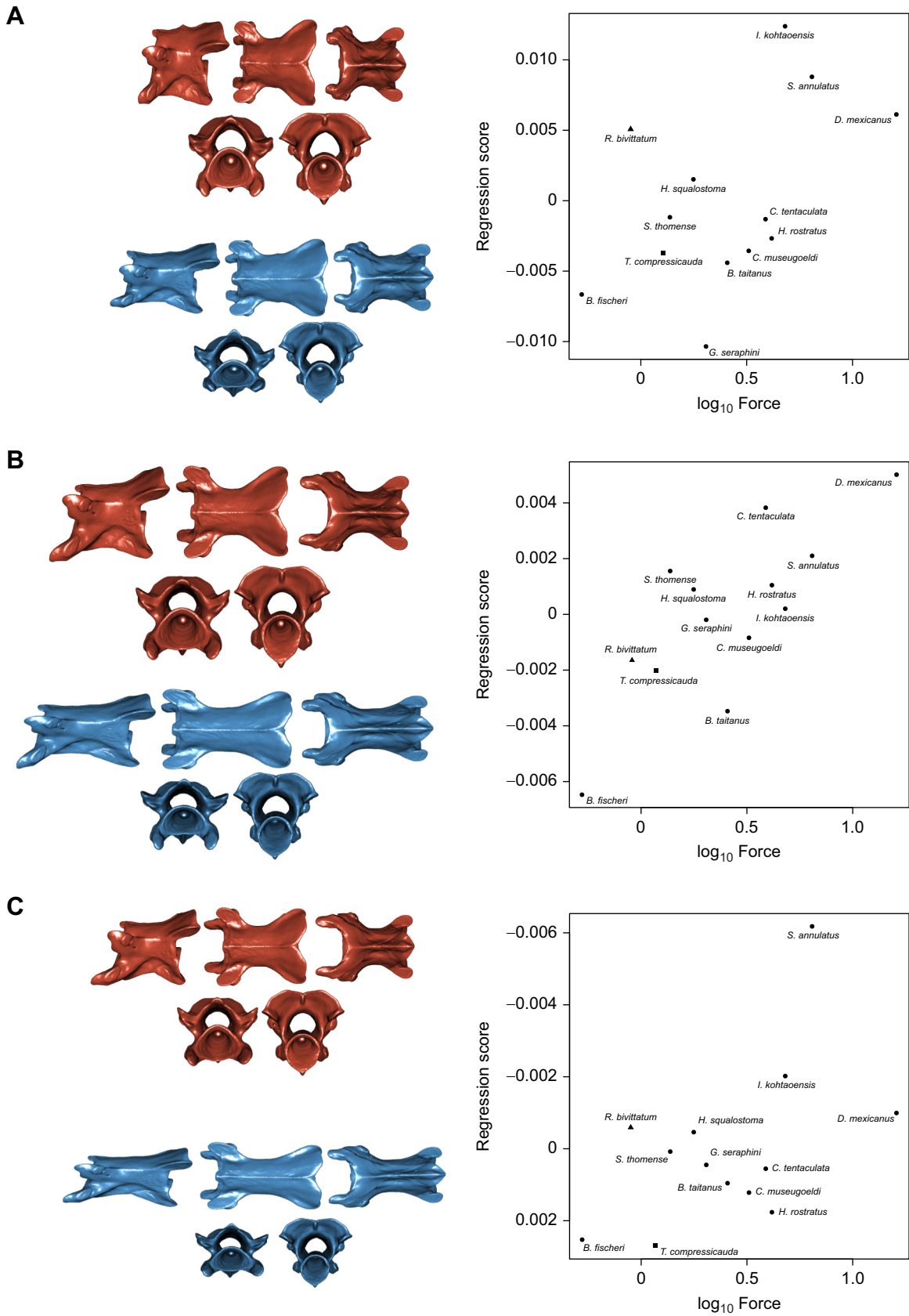


Fig. 2. See next page for legend.

**Fig. 2. Scatterplot of the phylogenetic generalized least squares (PGLS) regression showing the relationship between vertebral shape and maximal burrowing force in caecilians ( $n=120$ ).** (A) V3, (B) V20% and (C) V60%. Points represent species means ( $n=13$ ). Aquatic species are represented by squares, more surface-active species by triangles, and active burrowers rarely encountered on the surface by circles. Note that *I. kohtaoensis* may also be classified as a surface-active species, yet quantitative ecological data are rare and ecologies should be interpreted with caution. For full species names, see Table 1. Warped surfaces represent the shape variation associated with the maximum push force. The hypothetical shape associated with minimal push force extracted from the regression is illustrated in blue; the theoretical shape associated with maximum push force is in red. Top rows, from left to right: left lateral, dorsal and ventral views. Bottom rows, from left to right: anterior and posterior views.

monitored for signs of weight loss during the following weeks. None of the animals were harmed, or showed any signs of stress or weight loss after measurements, and all measurements were approved by local animal care and use committees.

## RESULTS

### Phylogenetic signal

The multivariate  $K$ -statistic calculated for vertebral shape was generally significant but the signal was moderate (V1:  $K_{\text{mult}}=0.72$ ,  $P=0.001$ ; V2:  $K_{\text{mult}}=0.78$ ,  $P=0.01$ ; V3:  $K_{\text{mult}}=0.74$ ,  $P=0.01$ ; V20%:  $K_{\text{mult}}=0.64$ ,  $P=0.01$ ; V60%:  $K_{\text{mult}}=0.69$ ,  $P=0.01$ ). However, no significant phylogenetic signal was detected for the shape of V90% ( $K_{\text{mult}}=0.54$ ,  $P=0.07$ ) or the maximal push force ( $K=0.66$ ,  $P=0.53$ ).

### Relationships between vertebral number, shape and force

Our PGLS regressions showed no significant relationship between vertebral shape and vertebral number (Table 3). However, the PGLS regressions did show a significant relationship between shape and burrowing force for V3, V20% and V60%, but not for the two most anterior vertebrae (V1 and V2) or V90% (Table 4). Overall, for the three vertebrae showing a significant relationship with push force, high forces were associated with vertebral shapes that were antero-posteriorly shorter and taller, combined with a widening and elevation of the posterior aspect of the neural arch. Additionally, high forces were associated with round anterior cotyles whereas low forces were associated with elliptical cotyles (Fig. 2).

Among the species examined, *Boulengerula fischeri* had the most elongated vertebrae and the lowest forces (Fig. 2). Additionally, the aquatic *Typhlonectes compressicauda* also showed relatively elongated V60% vertebrae with elliptical cotyles in association with low forces (Fig. 2C). For V3, *Ichthyophis kohtaoensis*, *Siphonops annulatus* and *Dermophis mexicanus* were the species that showed high burrowing forces associated with short and robust vertebrae (Fig. 2A). For V20% and V60%, high forces were mainly associated with short vertebrae and a large neural arch as found respectively in *D. mexicanus* and *S. annulatus* (Fig. 2B,C).

## DISCUSSION

One of the assumptions of our study is that burrowing forces generated and experienced by caecilians are relatively high, as suggested by previous studies (O'Reilly et al., 1997). Although until recently, comparative performance data from other head-first burrowing vertebrates were scarce, over the past few years, data on push forces obtained using similar protocols have been published for snakes (Herrel et al., 2021) and skinks (Le Guilloux et al., 2020). When comparing these taxa, caecilians appear to produce, on average, lower forces for a given body diameter than either burrowing snakes or skinks (Fig. 3; Table S2). Caution should be

made when interpreting these results as our dataset only comprises one caecilian with a true tail – *Rhinatrema bivittatum* (Nussbaum, 1977; Nussbaum and Wilkinson, 1989; Wake, 2003) – whereas all the skinks and snakes in our study have tails. During the experiments, some specimens were observed to bend the terminal end of their body to likely gain more grip, potentially impacting forward pushing force. As such, the tail could provide a force advantage in skinks and snakes. However, the only tailed terrestrial caecilian included in our analyses had the lowest force among the caecilians tested (Lowie et al., 2021), suggesting that tails may not be that important in generating forward force. Yet, despite these relatively low forces, our study shows that some of the variation in vertebral shape is correlated with maximal *in vivo* push forces. As no relationship was observed between the shape of the first two vertebrae and the maximal *in vivo* forces recorded, this suggests that external forces (reaction forces from the soil, encountered while extending the vertebral column) may not be high enough to significantly impact the shape of the anterior-most vertebrae. Overall, the first two vertebrae in caecilians are rather distinct compared with the other vertebrae (Lowie et al., 2022b; Peter, 1894; Taylor, 1977; Wake, 2003). Although rotation between the two first vertebrae seems limited in caecilians (Wake, 1980), they do appear to be modified for craniocervical movements (e.g. Hoffstetter and Gasc, 1969; Čeranský and Stanley, 2019). For instance, during initial soil penetration, the head angle is important in positioning the head for optimal soil penetration (Kleinteich et al., 2012). The head and the anterior part of the body are also implied in food capture and processing. Apart from rotational feeding (Measey and Herrel, 2006), caecilians also use head movements to tear apart their prey on

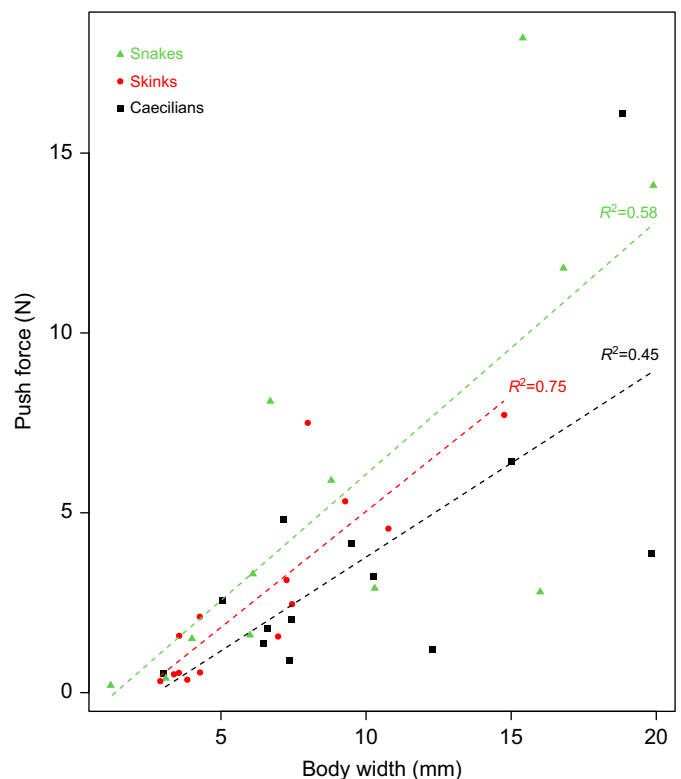


**Fig. 3. Scatterplot of the regression of mean body width against mean maximum push force in caecilians ( $N=13$ ), snakes ( $N=12$ ) and skinks ( $N=14$ ).** The data used for this plot were extracted from Herrel et al. (2021) for snakes, Le Guilloux et al. (2020) for skinks and this paper for caecilians. See Table S2 for the complete dataset used for this plot.

the surrounding walls of their burrows (Herrel and Measey, 2012). Consequently, other functional demands may be more important in driving the evolution of the shape of the first two vertebrae in caecilians. Interestingly, no link seems to exist between the total number of vertebrae and the shape of any given vertebra, suggesting that species with a different number of vertebrae can safely be compared with one another.

In contrast to the first two vertebrae, the mid-body vertebrae appear to be shaped by constraints incurred during locomotion (Lowie et al., 2022b; Wake, 1980). Our results show that the shape of V3, V20% and V60% is indeed related to the peak push force measured *in vivo*. However, external forces explain only a relatively small proportion (17–25%) of the variation in vertebral shape, with the shape of the more posterior mid-body vertebrae being more tightly associated with push force. Given (1) the relatively low push forces in caecilians, and (2) the absence of a relationship between push force and the shape of the two first vertebrae, we suggest that the observed relationship between vertebral shape and burrowing force reflects a functional link between axial muscle use during burrowing and vertebral shape, rather than the need for the vertebrae to withstand substrate reaction forces. To test this hypothesis, however, quantitative data on the axial musculature such as the volume or physiological cross-sectional area of the axial muscles obtained through dissection or contrast-enhanced  $\mu$ CT scans are needed.

As suggested previously, variation in stoutness of the body and vertebrae (with stouter vertebrae in species producing higher forces, e.g. *D. mexicanus* or *S. annulatus*) might be associated with differences in locomotor type and substrates used (Renous and Gasc, 1989; Renous et al., 1993). Our results show that species generally considered active burrowers such as *D. mexicanus* generate higher push forces and have short and bulky vertebrae. Moreover, as observed in *S. annulatus*, the articulatory facets of the zygapophyses are more obliquely oriented, likely increasing the imbrication between adjacent vertebrae, and thus the resistance of the vertebral column to torsion. In contrast, more surface-active species with low burrowing forces appear to have relatively longer vertebrae with more horizontally oriented processes.

Interestingly, the posterior-most vertebra included in our study (V90%) shows no relationship with peak push force. Although little difference in overall shape is observed between V60% and V90% (Lowie et al., 2022b), posterior vertebrae may have additional functional roles. Indeed, the correct positioning of the posterior region of the body is required during copulation (e.g. Kupfer et al., 2006). Moreover, during initial soil penetration, the posterior end of the body is also used to press against the substrate (M.W., personal observation), seemingly to gain purchase as animals push their heads into the soil. Such behaviors likely impose significantly different constraints on mobility and shape. Additionally, in aquatic species such as *T. compressicauda*, the posterior part of the body may act as a rudder and the increased rigidity provided by longer vertebrae could increase the efficiency of force transfer from the animal to the fluid.

## Conclusion

While the vertebrae in the anterior- and posterior-most parts of the vertebral column are likely shaped by multiple functions, and this shows no association with maximal forces measured *in vivo*, the rest of the vertebrae analyzed do show relationships with maximal push forces. Yet, these relationships are likely due to co-evolution of the axial musculature that attaches to these vertebrae, and the vertebral shape. Further anatomical studies on the axial musculature are

needed to fully understand the selective pressures acting on the post-cranial skeleton. Our results further suggest that isolated vertebrae recovered in the fossil record (e.g. Estes and Wake, 1972; Evans and Sigogneau-Russel, 2001; Rage, 1986) may be informative on the burrowing capacity of these species. This information may potentially allow for inference of the lifestyle of fossil caecilians and shed further light on the adaptive evolution of these secretive animals.

## Acknowledgements

We thank I. Josipovic and the people at Centre for X-Ray Tomography at Ghent University for their help with CT scanning. We thank the Museum of Zoology (University of Michigan), the Amphibian & Reptile Diversity Research Centre (University of Texas Arlington), the Royal Museum of Central Africa (Brussels) and the Zoological Museum (Hamburg), A. Kupfer and the Staatliches Museum für Naturkunde Stuttgart and all the curators in these institutions for the loan of some key specimens. We also thank MorphoSource for making scans available. A.L. thanks M. Segall for her helpful discussions on the statistical analyses, and also M. H. Wake for the gift of *Dermophis* specimens.

## Competing interests

The authors declare no competing or financial interests.

## Author contributions

Conceptualization: A.L., D.A., A.H.; Methodology: A.L.; Formal analysis: A.L.; Investigation: A.L.; Resources: A.L., M.W., J.M., J.C.O., N.J.K., P.G., J.B., T.K., A.H.; Data curation: B.D.K.; Writing - original draft: A.L.; Writing - review & editing: A.L., B.D.K., M.W., J.M., J.C.O., N.J.K., P.G., J.B., T.K., D.A., A.H.; Visualization: A.L.; Supervision: D.A., A.H.; Project administration: D.A., A.H.; Funding acquisition: A.L., J.M.

## Funding

This study was supported by the Research Foundation, Flanders (Fonds Wetenschappelijk Onderzoek, grant 11D5819N), a TOURNESOL travel grant, the Royal Belgian Zoological Society and a European Union Marie Curie Fellowship (HPMF-CT-2001-01407), and field work and visiting fellowship of the Fonds Wetenschappelijk Onderzoek, Flanders, Belgium (FWO-VI) to J.M. The special research fund of Ghent University (Bijzonder Onderzoeksfonds UGent) is acknowledged for financial support of the UGCT Centre of Expertise (BOF.EXP.2017.0007).

## References

- Adams, D. C. (2014). A generalized K statistic for estimating phylogenetic signal from shape and other high-dimensional multivariate data. *Syst. Biol.* **63**, 685–697. doi:10.1093/sysbio/syu030
- Bardua, C., Wilkinson, M., Gower, D. J., Sherratt, E. and Goswami, A. (2019). Morphological evolution and modularity of the caecilian skull. *BMC Evol. Biol.* **19**, 30. doi:10.1186/s12862-018-1342-7
- Blomberg, S. P., Garland, T. and Ives, A. R. (2003). Testing for phylogenetic signal in comparative data: behavioral traits are more labile. *Evolution* **57**, 717–745. doi:10.1111/j.0014-3820.2003.tb00285.x
- Čeranský, A. and Stanley, E. L. (2019). The atlas – axis complex in Dibamidae (Reptilia: Squamata) and their potential relatives: the effect of a fossorial lifestyle on the morphology of this skeletal bridge. *J. Morphol.* **280**, 1777–1797. doi:10.1002/jmor.21064
- Ducey, P. K., Formanowicz, D. R. J., Boyet, L., Mailloux, J. and Nussbaum, R. A. (1993). Experimental examination of burrowing behavior in caecilians (Amphibia: Gymnophiona): effects of soil compaction on burrowing ability of four species. *Herpetologica* **49**, 450–457.
- Dunn, E. R. (1942). The American caecilians. *Bull. Museum Comp. Zool.* **91**, 437–540.
- Estes, R. and Wake, M. H. (1972). The first fossil record of caecilian amphibians. *Nature* **239**, 228–231. doi:10.1038/239228b0
- Evans, S. E. and Sigogneau-Russel, D. (2001). A stem-group caecilian (Lissamphibia: Gymnophiona) from the lower Cretaceous of North Africa. *Paleontology* **44**, 259–273. doi:10.1111/1475-4983.00179
- Felsenstein, J. (1985). Phylogenies and the comparative method. *Am. Nat.* **125**, 1–15. doi:10.1086/284325
- Gans, C. (1973). Locomotion and burrowing in limbless vertebrates. *Nature* **242**, 414–415. doi:10.1038/242414a0
- Gaymer, R. (1971). New method of locomotion in limbless terrestrial vertebrates. *Nature* **234**, 150–151. doi:10.1038/234150a0
- Herrel, A. and Measey, G. J. (2010). The kinematics of locomotion in caecilians: effects of substrate and body shape. *J. Exp. Zool. Part A Ecol. Genet. Physiol.* **313A**, 301–309. doi:10.1002/jez.599

- Herrel, A. and Measey, G. J.** (2012). Feeding underground: kinematics of feeding in caecilians. *J. Exp. Zool. A Ecol. Genet. Physiol.* **317**, 533-539. doi:10.1002/jez.1745
- Herrel, A., Lowie, A., Miralles, A., Gaucher, P., Kley, N. J., Measey, J. and Tolley, K. A.** (2021). Burrowing in blindsnakes: a preliminary analysis of burrowing forces and consequences for the evolution of morphology. *Anat. Rec.* **304**, 2292-2302. doi:10.1002/ar.24686
- Hoffstetter, P. and Gasc, J. P.** (1969). Vertebrae and ribs of modern reptiles. In *Biology of the Reptilia. Volume 1. Morphology A.* (ed. C. Gans), pp. 201-210. New-York, USA: Academic Press.
- Jetz, W. and Pyron, R. A.** (2018). The interplay of past diversification and evolution of the skull of caecilians (Lissamphibia: Gymnophiona). *Proc. SPIE* **7078**, *Developments in X-Ray Tomography VI*, 70780D. doi:10.1117/12.795063
- Kleinteich, T., Beckmann, F., Herzen, J., Summers, A. P. and Haas, A.** (2008). Applying x-ray tomography in the field of vertebrate biology: form, function, and evolution of the skull of caecilians (Lissamphibia: Gymnophiona). *Proc. SPIE* **7078**, *Developments in X-Ray Tomography VI*, 70780D. doi:10.1117/12.795063
- Kleinteich, T., Maddin, H. C., Herzen, J., Beckmann, F. and Summers, A. P.** (2012). Is solid always best? Cranial performance in solid and fenestrated caecilian skulls. *J. Exp. Biol.* **215**, 833-844. doi:10.1242/jeb.065979
- Kupfer, A.** (2009). Sexual size dimorphism in caecilian amphibians: analysis, review and directions for future research. *Zoology* **112**, 362-369. doi:10.1016/j.zool.2008.12.001
- Kupfer, A., Kramer, A., Himstedt, W. and Greven, H.** (2006). Copulation and egg retention in an oviparous Caecilian (Amphibia: Gymnophiona). *Zool. Anz.* **244**, 223-228. doi:10.1016/j.jcz.2005.12.001
- Le Guilloux, M., Miralles, A., Measey, J., Vanhooydonck, B., O'Reilly, J., Lowie, A. and Herrel, A.** (2020). Trade-offs between burrowing and biting force in fossorial scincid lizards? *Biol. J. Linn. Soc.* **130**, 310-319. doi:10.1093/biolinnean/blaa031
- Lowie, A., De Kegel, B., Wilkinson, M., Measey, J., O'Reilly, J. C., Kley, N. J., Gaucher, P., Brecko, J., Kleinteich, T., Van Hoorebeke, L. et al.** (2021). Under pressure: the relationship between cranial shape and burrowing force in caecilians (Gymnophiona). *J. Exp. Biol.* **224**, jeb242964. doi:10.1242/jeb.242964
- Lowie, A., De Kegel, B., Wilkinson, M., Measey, J., O'Reilly, J. C., Kley, N. J., Gaucher, P., Brecko, J., Kleinteich, T., Adriaens, D. et al.** (2022a). The relationship between head shape, head musculature and bite force in caecilians (Amphibia: Gymnophiona). *J. Exp. Biol.* **225**, jeb243599. doi:10.1242/jeb.243599
- Lowie, A., De Kegel, B., Wilkinson, M., Measey, J., O'Reilly, J. C., Kley, N. J., Gaucher, P., Brecko, J., Kleinteich, T., Herrel, A. et al.** (2022b). Regional differences in vertebral shape along the axial skeleton in caecilians (Amphibia: Gymnophiona). *J. Anat.* doi:10.1111/joa.13682
- Maddock, S. T., Wilkinson, M., Nussbaum, R. A. Gower, D. J.** (2017). A new species of small and highly abbreviated caecilian (Gymnophiona: Indotyphlidae) from the Seychelles island of Praslin, and a recharacterization of *Hypogeophis brevis* Boulenger, 1911. *Zootaxa* **4329**, 301-326. doi:10.11646/zootaxa.4329.4.1
- Maerker, M., Reinhard, S., Pogoda, P. and Kupfer, A.** (2016). Sexual size dimorphism in the viviparous caecilian amphibian *Geotrypetes seraphini* seraphini (Gymnophiona: Dermophiidae) including an updated overview of sexual dimorphism in caecilian amphibians. *Amphib. Reptil.* **37**, 291-299. doi:10.1163/15685381-00003057
- Masschaele, B., Dierick, M., Van Loo, D., Boone, M. N., Brabant, L., Pauwels, E., Cnudde, V. and Van Hoorebeke, L.** (2013). HECTOR: A 240kV micro-CT setup optimized for research. *J. Phys. Conf. Ser.* **463**, 012012. doi:10.1088/1742-6596/463/1/012012
- Measey, G. J. and Herrel, A.** (2006). Rotational feeding in caecilians: putting a spin on the evolution of cranial design. *Biol. Lett.* **2**, 485-487. doi:10.1098/rsbl.2006.0516
- Naylor, B. G. and Nussbaum, R. A.** (1980). The trunk musculature of caecilians (Amphibia: Gymnophiona). *J. Morphol.* **166**, 259-273. doi:10.1002/jmor.1051660302
- Nussbaum, R. A.** (1977). Rhinatrematidae: A new family of caecilians (Amphibia: Gymnophiona). *Occas. Pap. Museum Zool.* **682**, 1-30.
- Nussbaum, R. A. and Naylor, B. G.** (1982). Variation in the trunk musculature of caecilians (Amphibia: Gymnophiona). *J. Zool.* **198**, 383-398. doi:10.1111/j.1469-7998.1982.tb02083.x
- Nussbaum, R. A. and Pfrender, M. E.** (1998). Revision of the African caecilian genus *Schistometopum* Parker (Amphibia: Gymnophiona: Caeciliidae). *Misc. Publ. Museum Zool. Univ. Michigan* **187**, 1-32.
- Nussbaum, R. A. and Wilkinson, M.** (1989). On the classification and phylogeny of caecilians (Amphibia: Gymnophiona), a critical review. *Herpetol. Monogr.* **3**, 1-42. doi:10.2307/1466984
- O'Reilly, J. C.** (2000). Feeding in caecilians. In *Feeding: Form, Function, and Evolution in Tetrapod Vertebrates* (ed. K. Schwenk), pp. 149-166. Academic Press.
- O'Reilly, J. C., Ritter, D. A. and Carrier, D. R.** (1997). Hydrostatic locomotion in a limbless tetrapod. *Nature* **386**, 269-272. doi:10.1038/386269a0
- Peter, K.** (1894). Die Wirbelsäule der Gymnophionen. *Ber. Naturforsch. Ges. Freiburg.* **9**, 35-58.
- Rage, J.-C.** (1986). Le plus ancien amphibien apode (Gymnophiona) fossile. Remarques sur la répartition et l'histoire paléobiogéographique des gymnophiones. *Acad. Sci.* **302**, 1033-1036.
- Renous, S. and Gasc, J.-P.** (1989). Body and vertebral proportions in Gymnophiona (Amphibia): diversity of morphological types. *Copeia* **1989**, 837-847. doi:10.2307/1445966
- Renous, S., Gasc, J.-P. and Ineich, I.** (1993). Données préliminaires sur les capacités locomotrices des amphibiens gymnophiones. *Ann. Sci. Nat.* **14**, 59-79.
- Sherratt, E., Gower, D. J., Klingenberg, C. P. and Wilkinson, M.** (2014). Evolution of cranial shape in caecilians (Amphibia: Gymnophiona). *Evol. Biol.* **41**, 528-545. doi:10.1007/s11692-014-9287-2
- Summers, A. P. and O'Reilly, J. C.** (1997). A comparative study of locomotion in the caecilians *Dermophis mexicanus* and *Typhlonectes natans* (Amphibia: Gymnophiona). *Zool. J. Linn. Soc.* **121**, 65-76. doi:10.1111/j.1096-3642.1997.tb00147.x
- Taylor, E. H.** (1968). *The Caecilians of the World. A Taxonomic Review.* Lawrence: University of Kansas Press.
- Taylor, E. H.** (1977). Comparative anatomy of caecilian anterior vertebrae. *Univ. Kansas Sci. Bull.* **51**, 219-231. doi:10.5962/bhl.part.24959
- Vanhooydonck, B., Boistel, R., Fernandez, V. and Herrel, A.** (2011). Push and bite: trade-offs between burrowing and biting in a burrowing skink (*Acontias percivali*). *Biol. J. Linn. Soc.* **101**, 461-475. doi:10.1111/j.1095-8312.2010.01519.x
- Wake, M. H.** (1980). Morphometrics of the skeleton of *Dermophis mexicanus* (Amphibia Gymnophiona). Part I. The vertebrae, with comparisons to other species. *J. Morphol.* **165**, 117-130. doi:10.1002/jmor.1051650202
- Wake, M. H.** (1993). The skull as a locomotor organ. In *The Skull: Functional and Evolutionary Mechanisms* (ed. J. Hanken and B. K. Hall), pp. 197-240. Chicago, IL, USA: University of Chicago Press.
- Wake, M. H.** (2003). The osteology of caecilians. In *Amphibian Biology, Volume 5. Osteology* (ed. H. Heatwole and M. Davies), pp. 1809-1876. Chipping Norton, NSW: Surrey Beatty and Sons.
- Wake, M. H. and Hanken, J.** (1982). Development of the skull of *Dermophis mexicanus* (Amphibia: Gymnophiona), with comments on skull kinesis and amphibian relationships. *J. Morphol.* **173**, 203-223. doi:10.1002/jmor.1051730208
- Wiedersheim, R.** (1879). *Die Anatomie der Gymnophionen.* Jena: Gustav Fischer.
- Wilkinson, M.** (2012). Caecilians. *Curr. Biol.* **22**, R668-R669. doi:10.1016/j.cub.2012.06.019
- Wilkinson, M. and Nussbaum, R. A.** (1997). Comparative morphology and evolution of the lungless caecilian *Atretochoana eiselti* (Taylor) (Amphibia: Gymnophiona: Typhlonectidae). *Biol. J. Linn. Soc.* **62**, 39-109. doi:10.1111/j.1095-8312.1997.tb01616.x

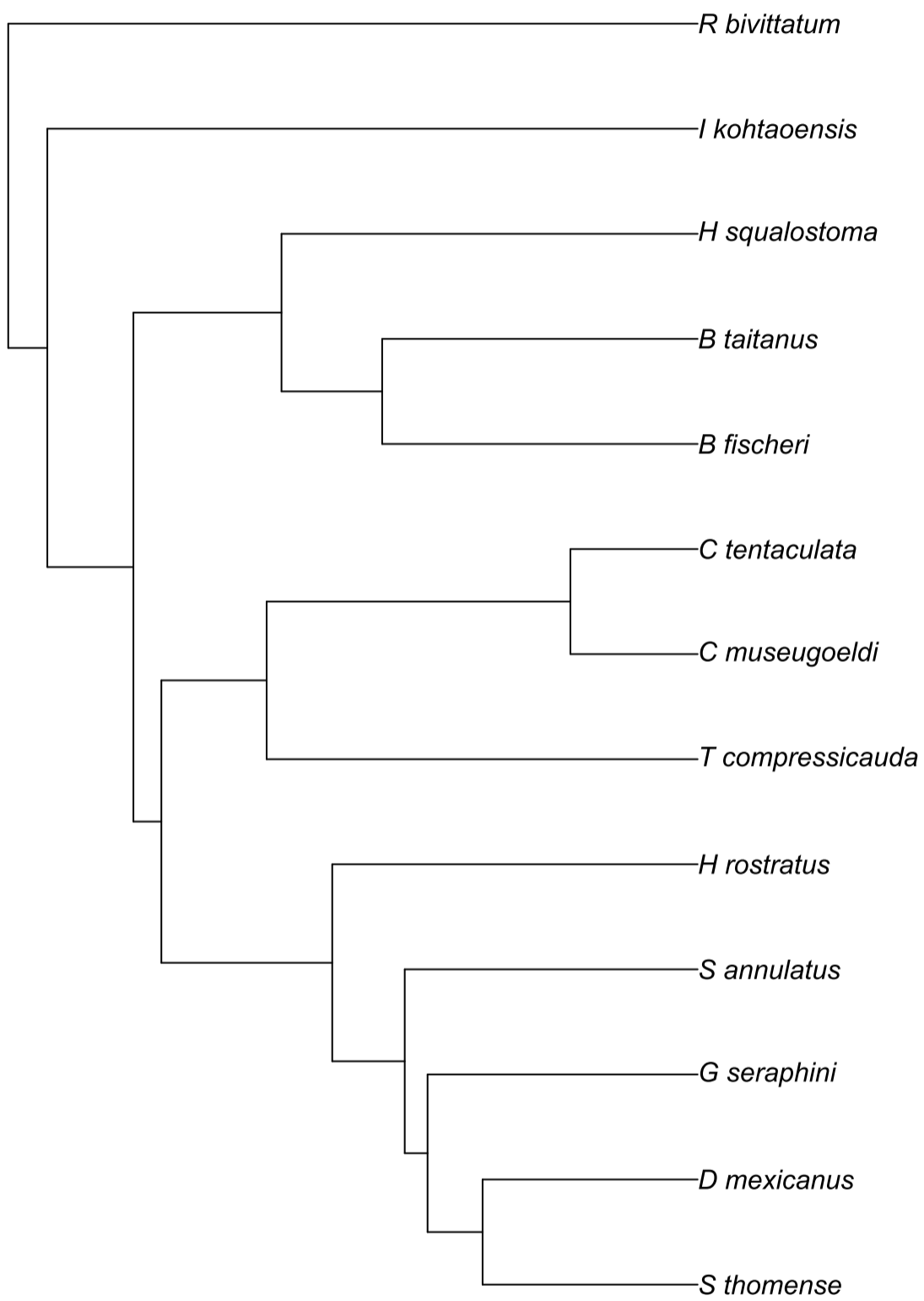


**Fig. S1.** Maximum credibility tree used in our analyses



**Table S1.** Details of the specimens/scans used in the study.

Family	Species	ID	Origin	Voxel size (μm)
Rhinatremaidae	<i>Rhinatrema bivittatum</i> <sup>†</sup>	Rhinatrema bivittatum byu:main:48675	MS	12.81
	<i>Rhinatrema bivittatum</i> <sup>*</sup>	Rhinatrema bivittatum A53	AH	31.72
	<i>Rhinatrema bivittatum</i> <sup>*†</sup>	Rhinatrema bivittatum AL8	AH	31.72
	<i>Rhinatrema bivittatum</i> <sup>*</sup>	Rhinatrema bivittatum B75	AH	33.07
	<i>Rhinatrema bivittatum</i> <sup>*</sup>	Rhinatrema bivittatum B80	AH	28.34
Ichthyophiidae	<i>Ichthyophis kohtaoensis</i>	Ichthyophis kohtaoensis ncsm:herp:7920	MS	18.01
	<i>Ichthyophis kohtaoensis</i> <sup>†</sup>	Ichthyophis kohtaoensis ZMH A08981	ZMH	6.83
	<i>Ichthyophis kohtaoensis</i> <sup>*</sup>	Ichthyophis kohtaoensis 218831	UMMZ	31.72
	<i>Ichthyophis kohtaoensis</i> <sup>*</sup>	Ichthyophis kohtaoensis 218832	UMMZ	31.72
Herpelidae	<i>Boulengerula fischeri</i> <sup>*</sup>	Boulengerula fischeri 3	AH	32.48
	<i>Boulengerula fischeri</i> <sup>*</sup>	Boulengerula fischeri 4	AH	32.48
	<i>Boulengerula fischeri</i> <sup>*</sup>	Boulengerula fischeri 5	AH	32.48
	<i>Boulengerula fischeri</i> <sup>*</sup>	Boulengerula fischeri 7	AH	32.48
	<i>Boulengerula fischeri</i> <sup>*†</sup>	Boulengerula fischeri AH1	AH	9.74
	<i>Boulengerula taitanus</i> <sup>*†</sup>	Boulengerula taitanus AH2	AH	16.07
	<i>Boulengerula taitanus</i> <sup>*</sup>	Boulengerula taitanus AL010401	AH	31.72
	<i>Boulengerula taitanus</i> <sup>*†</sup>	Boulengerula taitanus AL010402	AH	9.74
	<i>Boulengerula taitanus</i> <sup>*</sup>	Boulengerula taitanus JM01452	AH	33.07
	<i>Boulengerula taitanus</i> <sup>*</sup>	Boulengerula taitanus JM01584	AH	33.07
	<i>Herpele squalostoma</i> <sup>*</sup>	Herpele squalostoma AL10	AH	34.37
	<i>Herpele squalostoma</i> <sup>*</sup>	Herpele squalostoma AL2	AH	31.72
	<i>Herpele squalostoma</i> <sup>*</sup>	Herpele squalostoma AL30	AH	31.72
	<i>Herpele squalostoma</i> <sup>*</sup>	Herpele squalostoma AL31	AH	34.35
	<i>Herpele squalostoma</i> <sup>*</sup>	Herpele squalostoma AL32	AH	32.48
Caeciliidae	<i>Caecilia museugoeldi</i> <sup>*</sup>	Caecilia museugoeldi V2101	NHM	63.47
	<i>Caecilia tentaculata</i> <sup>*</sup>	Caecilia tentaculata 3955	NHM	90.83
	<i>Caecilia tentaculata</i>	Caecilia tentaculata ku:kuh:175441	MS	77.33
Typhlonectidae	<i>Typhlonectes compressicauda</i> <sup>†</sup>	Typhlonectes compressicauda 11307	NHM	8.4
	<i>Typhlonectes compressicauda</i>	Typhlonectes compressicauda cas:herp:12542	MS	36.87
	<i>Typhlonectes compressicauda</i> <sup>*</sup>	Typhlonectes compressicauda AL20	AH	17.65
	<i>Typhlonectes compressicauda</i> <sup>*</sup>	Typhlonectes compressicauda AL6	AH	49.37

Indotyphliidae	<i>Typhlonectes compressicauda</i> *†	Typhlonectes compressicauda AL7	AH	46.81
	<i>Hypogeophis rostratus</i>	Hypogeophis rostratus 73_38_B_101	RMCA	20.99
	<i>Hypogeophis rostratus</i>	Hypogeophis rostratus 73_38_B_110	RMCA	20.99
	<i>Hypogeophis rostratus</i>	Hypogeophis rostratus 73_38_B_111	RMCA	25.94
	<i>Hypogeophis rostratus</i> †	Hypogeophis rostratus 73_48_B_1	RMCA	19.01
Siphonopidae	<i>Siphonops annulatus</i>	Siphonops annulatus cas:herp:74304	MS	22.17
	<i>Siphonops annulatus</i> †	Siphonops annulatus 1924_9_20_9_Red	NHM	9.82
	<i>Siphonops annulatus</i> †	Siphonops annulatus ZMH A00235	ZMH	9.2
Dermophiidae	<i>Dermophis mexicanus</i>	Dermophis mexicanus cas:herp:144523	MS	50.79
	<i>Dermophis mexicanus</i> *	Dermophis mexicanus A-52188	UTACV	56.04
	<i>Dermophis mexicanus</i> *	Dermophis mexicanus AL2101201	AL	88.52
	<i>Dermophis mexicanus</i> *	Dermophis mexicanus AL2101202	AL	93.79
	<i>Geotrypetes seraphini</i> *†	Geotrypetes seraphini AL29041901	AL	49.37
	<i>Geotrypetes seraphini</i> *	Geotrypetes seraphini 2	AH	49.37
	<i>Geotrypetes seraphini</i> *†	Geotrypetes seraphini 6	AH	15.17
	<i>Geotrypetes seraphini</i> *	Geotrypetes seraphini AL1	AH	16
	<i>Geotrypetes seraphini</i> *	Geotrypetes seraphini AL21	AH	56.62
	<i>Geotrypetes seraphini</i> *	Geotrypetes seraphini AL5	AH	35.94
	<i>Schistometopum thomense</i> *	Schistometopum thomense 6	AH	32.48
	<i>Schistometopum thomense</i> *	Schistometopum thomense 7	AH	32.48
	<i>Schistometopum thomense</i> *	Schistometopum thomense #8	AH	32.48
	<i>Schistometopum thomense</i> *	Schistometopum thomense AL11	AH	32.48

\*Specimens scanned using the HECTOR micro computed tomography ( $\mu$ CT) scanner

†Specimens for which only the atlas was available

Abbreviations are as follows:

- Personal collection of Anthony Herrel (AH)
- Personal collection of Aurélien Lowie (AL)
- Morphosource.org (MS)
- Natural History Museum, London (NHM)
- Royal Museum of Central Africa (RMCA)
- Staatliches Museum für Naturkunde Stuttgart (SMNS)
- University of Michigan, Museum of Zoology (UMMZ)
- University of Texas Arlington, Amphibian & Reptile Diversity Research Center (UTACV)
- Zoological Museum, Hamburg (ZMH)

**Table S2. Body width, push force and supposed ecology of the skinks, snakes and caecilians used in this study.**

	Species	Body width (mm)	Push force (N)	Ecology
Skinks	<i>Acontias kgalagadi</i>	4.28	0.56	Active burrower
	<i>Acontias litoralis</i>	3.38	0.51	Active burrower
	<i>Acontias meleagris</i>	7.26	3.13	Active burrower
	<i>Acontias percivali</i>	9.28	5.32	Active burrower
	<i>Chalcides ocellatus</i>	10.77	4.56	leaf litter
	<i>Chalcides sepsoides</i>	7.45	2.46	sand swimmer
	<i>Mochlus sundevallii</i>	6.97	1.56	leaf litter
	<i>Pygomeles braconnieri</i>	7.99	7.5	sand swimmer
	<i>Scelotes bipes</i>	3.84	0.36	Active burrower
	<i>Scelotes montispectus</i>	3.55	0.55	Active burrower
	<i>Scincus scincus</i>	14.76	7.72	sand swimmer
	<i>Typhlosaurus caecus</i>	4.27	2.11	Active burrower
	<i>Typhlosaurus lomiae</i>	2.91	0.32	Active burrower
<i>Typhlosaurus vermis</i>	3.56	1.58	Active burrower	
Snakes	<i>Anilius scytale</i>	8.8	5.9	leaf litter
	<i>Aparallactus guentheri</i>	6	1.6	leaf litter
	<i>Eryx colubrinus</i>	16	2.8	Active burrower
	<i>Farancia abacura</i>	16.8	11.8	Active burrower
	<i>Loxocemus bicolor</i>	19.9	14.1	Active burrower
	<i>Oxyrhopus melanogerys</i>	10.3	2.9	leaf litter
	<i>Afrotyphlos angolensis</i>	15.4	18.2	Active burrower
	<i>Rhinothyphlos lalandei</i>	6.1	3.3	Active burrower
	<i>Rhinotyphlops unitaeniatus</i>	6.7	8.1	Active burrower
	<i>Leptotyphlops scutifrons</i>	3.1	0.4	Active burrower
	<i>Myriopholis algeriensis</i>	1.2	0.2	uses existing burrows
<i>Liotyphlops beui</i>	4	1.5	uses existing burrows	
Caecilians	<i>Boulengerula fischeri</i>	3.02	0.53	Active burrower
	<i>Boulengerula taitanus</i>	5.04	2.56	Active burrower
	<i>Caecilia museugoeldi</i>	10.24	3.23	Active burrower
	<i>Caecilia tentaculata</i>	19.84	3.88	Active burrower
	<i>Dermophis mexicanus</i>	18.85	16.11	Active burrower
	<i>Geotrypetes seraphini</i>	7.43	2.03	Active burrower
	<i>Herpele squalostoma</i>	6.6	1.77	Active burrower
	<i>Hypogeophis rostratus</i>	9.5	4.15	Active burrower
	<i>Ichthyophis kohtaoensis</i>	7.15	4.8	leaf litter
	<i>Rhinatrema bivittatum</i>	7.37	0.89	leaf litter
	<i>Schistometopum thomense</i>	6.47	1.37	leaf litter
	<i>Siphonops annulatus</i>	15	6.43	Active burrower
	<i>Typhlonectes compressicauda</i>	12.28	1.19	Aquatic

Data were extracted from Herrel *et al.* (2021) for snakes, Le Guilloux *et al.* (2021) for skinks and this paper for caecilians.